

Phase Transition in a Non-Markovian Animal Exploration Model with Preferential Returns

Ohad Vilk^{1,2,3}, Daniel Campos,⁴ Vicenç Méndez⁴, Emmanuel Lourie^{2,3},
Ran Nathan^{2,3} and Michael Assaf^{1,5,*}

¹*Racah Institute of Physics, The Hebrew University of Jerusalem, Jerusalem 91904, Israel*

²*Movement Ecology Lab, Department of Ecology, Evolution and Behavior, Alexander Silberman Institute of Life Sciences, Faculty of Science, The Hebrew University of Jerusalem, Jerusalem 91904, Israel*

³*Minerva Center for Movement Ecology, The Hebrew University of Jerusalem, Jerusalem 91904, Israel*

⁴*Grup de Física Estadística, Dept. de Física, Universitat Autònoma de Barcelona, 08193 Bellaterra (Barcelona), Spain*

⁵*Institute for Physics and Astronomy, University of Potsdam, Potsdam 14476, Germany*



(Received 23 November 2021; accepted 16 February 2022; published 5 April 2022)

We study a non-Markovian and nonstationary model of animal mobility incorporating both exploration and memory in the form of preferential returns. Exact results for the probability of visiting a given number of sites are derived and a practical WKB approximation to treat the nonstationary problem is developed. A mean-field version of this model, first suggested by Song *et al.*, [Modelling the scaling properties of human mobility, *Nat. Phys.* **6**, 818 (2010)] was shown to well describe human movement data. We show that our generalized model adequately describes empirical movement data of Egyptian fruit bats (*Rousettus aegyptiacus*) when accounting for interindividual variation in the population. We also study the probability of visiting any site a given number of times and derive a mean-field equation. Our analysis yields a remarkable phase transition occurring at preferential returns which scale linearly with past visits. Following empirical evidence, we suggest that this phase transition reflects a trade-off between extensive and intensive foraging modes.

DOI: [10.1103/PhysRevLett.128.148301](https://doi.org/10.1103/PhysRevLett.128.148301)

Introduction.—Movement is a vital part of life and is key in a wide range of physical, biological, and ecological systems. Theoretical and empirical frameworks are thus amply used to study the mechanisms underlying movement patterns in all organisms [1]. In particular, individual-based modeling of movement has played a crucial role in studying dynamic systems across multiple spatiotemporal scales [2–4]. These models can be applied to infer behaviors and draw causal links between observed phenomena and their underlying mechanisms beyond phenomenological description of the observed patterns [5].

Most theoretical models assume Markovianity to capture the properties of animal trajectories. Yet memory and similar cognitive mechanisms are key to understanding patterns observed in animal foraging [6,7]. A range of taxa, from insects to primates, were shown to exhibit spatial learning and memory, and researchers have just begun to understand how to experimentally measure and control such effects [8]. While memory can appear at many different levels in this context (risk-avoidance, habituation, social learning, ...), the tendency of many organisms to repeatedly return to previously visited sites as a part of their regular foraging strategies represent a paradigmatic example. This has been recurrently observed for many species [4,9–12], and stochastic models have been proposed to justify how organisms store and manage cognitive information during that process [13].

Notably, memory patterns must be properly balanced by the organisms with some level of behavioral plasticity to enhance flexibility and exploration (see, e.g., Ref. [14]). For all these reasons, correctly incorporating memory within stochastic models is an important research line for improving both predictive and descriptive tools of movement [6,15–17]. Indeed, it has been shown that heuristic models of memory can be derived from microscopic consideration for limited cases [18,19]. At the same time, new experimental methods are allowing to disentangle, even under field conditions, memory effects on movement from other cognitive or perception mechanisms [10,20]. As long as such experimental and theoretical advances can nourish each other, new levels of detail in our understanding of living organisms can be potentially reached.

Dealing with memory and similar cognitive mechanisms still represents a significant theoretical challenge. Stochastic models that allow the individual to return to its original position (resettings) have attracted much attention recently [21–23], but these only incorporate memory in an elementary way. More complex self-avoiding random walks or preferential returns (PR), where the individual returns to any previous location with a probability proportional to the number of previous visits have also been studied [24–28]. These models are non-Markovian (and

typically also nonstationary), requiring that the individual identifies and keeps record of its entire trajectory. While the propagator of these models [29], and some properties of relocation times [30], have been computed, characterizing the revisits complete statistics to each particular location remains an open problem.

Here we study a non-Markovian and nonstationary mechanistic model of animal mobility, explicitly incorporating both the tendency of an individual to return to previously visited locations (PR) and the tendency to explore new sites. Versions of this model have been used to model the mobility of humans [24] and monkeys [31], the latter suggesting that monkey movement is nonrandom due to the use of memory and visitation patterns driven by resource availability. We generalize the model by accounting for stochasticity, incorporating interspecific variability in the population, and allowing for nonlinear PR [32]. We provide analytical solutions to this non-Markovian, nonstationary model that go well beyond previous *mean-field* results. In particular, we present several approaches to analytically find the probability of having visited n sites at time t and study the statistics of how revisits are distributed through the available locations. Our approach, based on the Wentzel-Kramers-Brillouin (WKB) approximation, is thus useful to deal with explicitly time-dependent problems. Remarkably, by allowing for nonlinear PR we find a phase transition as a function of the strength of the PR, where above some threshold the most visited site dominates the dynamics, receiving practically all new visits. We suggest that this phase transition reflects a balance between the tendency to return to known sites and the will to explore new ones [22]. Our predictions are verified using simulations, and are shown to adequately describe the space use patterns and the revisitation dynamics of Egyptian fruit bats (*Rousettus aegyptiacus*) to fruit trees.

Model.—Our model includes (i) exploration—with probability P_{new} the animal visits a new site, and (ii) PR—with probability $1 - P_{\text{new}}$ the animal visits a previously visited site i with probability $\Pi_i(m_i)$, where m_i is the number of previous visits to site i . Following empirical data in humans and animals [24,31] we assume

$$P_{\text{new}} = qn^{-\beta}, \quad \Pi_i(m_i) = \frac{m_i^\alpha}{\sum_{j=1}^n m_j^\alpha}. \quad (1)$$

Here n is the number of previously visited sites, and $\beta > 0$ and $0 < q < 1$ control the animal's tendency to visit new sites indicating a power-law decay controlled by *conformity exponent* β . On the other hand, the PR exponent $\alpha > 0$, governs the tendency to return to a previously visited location. Furthermore, and without loss of generality, we order the sites by rank such that $i = 1$ is the most visited site with m_1 visits. Notably, we assume that the number of available sites is unbounded.

Cumulative number of sites.—The probability $P(n, t)$ of having visited n sites in $t \gg 1$ time steps follows

$$\partial P(n, t)/\partial t = q(n-1)^{-\beta}P(n-1, t) - qn^{-\beta}P(n, t), \quad (2)$$

with initial condition $P(n, 0) = \delta_{n,1}$. Although this *master equation* is interpreted here in the context of movement between spatially distributed sites, it can equivalently describe a birth-death process of population of size n , where the growth rate is proportional to $n^{-\beta}$ [33]. In particular, for $\beta = 0$ the birth-death process is $\emptyset \xrightarrow{q} A$ and for $\beta = -1$ the birth-death process is $A \xrightarrow{q} 2A$. While these special cases have known exact solutions, in this Letter we are primarily interested in the regime $\beta > 0$, which describes a growth which *decreases* [or saturates, see Eq. (1)] with the number of sites (or population size). To the best of our knowledge this regime has not been analytically studied.

An equation for the first moment $\langle n \rangle = \sum_n nP(n, t)$ can be obtained from Eq. (2) by multiplying the latter by n , summing over all n 's, and using the definition for $\langle n \rangle$. This yields $d\langle n \rangle/dt = q\langle n^{-\beta} \rangle$, which under the mean-field approximation $\langle n^{-\beta} \rangle \simeq \langle n \rangle^{-\beta}$ is solved by

$$\langle n \rangle = [(1 + \beta)qt]^{1/(1+\beta)}, \quad (3)$$

predicting a power-law dependence on the time of measurement, in agreement with Ref. [24]. A similar derivation for the second moment yields $\langle n^2 \rangle = \langle n \rangle^2 + \langle n \rangle$ such that the variance follows $\sigma_n^2 \equiv \langle n^2 \rangle - \langle n \rangle^2 = \langle n \rangle$, i.e., the variance of the number of sites is equal to the mean as in a Poisson process. This result, however, turns out to be inaccurate as it involves various uncontrolled assumptions, and is not consistent with simulations, as elaborated below.

An exact solution to Eq. (2) can be found by Laplace transforming it and solving the resulting recurrence equation [36]. The exact solution for $\beta \neq 0$ has the form (see Supplemental Material, Sec. S1A [37])

$$P(n, t) = (-1)^{n-1} n^\beta \sum_{k=1}^n \frac{k^{-\beta} e^{-qt/k^\beta}}{\prod_{j=1, j \neq k}^n (\frac{j^\beta}{k^\beta} - 1)}. \quad (4)$$

For special values of β this result simplifies to

$$P(n, t) = \begin{cases} e^{-nqt} (e^{qt} - 1)^{n-1} & \beta = -1 \\ \frac{1}{(n-1)!} (qt)^{n-1} e^{-qt} & \beta = 0 \\ \frac{1}{(n-1)!} \sum_{k=1}^n \binom{n}{k} (-1)^{n-k} k^{n-1} e^{-\frac{qt}{k}} & \beta = 1 \end{cases}. \quad (5)$$

Though Eq. (4) is an exact solution, it is given as a sum of large terms of alternating sign, which converges due to a precise balance between the terms. Thus, in practice this convergence is very slow for $n \gg 1$, and may result in a

significant loss of accuracy when evaluated numerically [42]. To circumvent these issues, we develop a time-dependent WKB approximation.

Time dependent WKB.—In the limit of a large number of sites $n \gg 1$, we substitute the time-dependent ansatz $P(n, t) \sim e^{-S(n, t)}$ into Eq. (2) [43–45]. Neglecting terms of order $\mathcal{O}(n^{-1})$, in the leading order we obtain a classical Hamilton-Jacobi equation for the action function $S(n, t): \partial_t S = H(n, \partial_n S) \equiv H(n, p)$, where we have defined the Hamiltonian $H(n, p) = q(1 - e^{-p})n^{-\beta}$, and denoted $p = -\partial_n S$ as the conjugate momentum. Instead of directly solving the Hamilton-Jacobi equation, we use the Hamilton approach for the classical equations of motion

$$\dot{n} = qe^{-p}n^{-\beta}, \quad \dot{p} = \beta q(1 - e^{-p})n^{-\beta-1}. \quad (6)$$

We write the action on a classical trajectory as [44] $S(n, t) = Et - \int^n p(n')dn'$, where the energy $E \equiv H[n(t), p(t)]$ is constant along a dynamical trajectory given by $p(n) = \log[q/(q - En^\beta)]$. To find the energy we solve Eq. (6) for \dot{n} on a given constant-energy dynamical trajectory. This yields (Supplemental Material, Sec. S1C [37])

$$P(n, t) \sim e^{-(n)S(x)},$$

$$S(x) = \frac{f(x)x^{-\beta}}{\beta + 1} + xf(x)^{-1/\beta}B[f(x); 1 + 1/\beta, 0] + x \log[1 - f(x)], \quad (7)$$

with $x \equiv n/\langle n \rangle$ and $f(x) = 1 - x^\beta[\beta(x - 1) + x]$. Here, $B[z; a, b] = \int_0^z u^{a-1}(1-u)^{b-1}du$ is the incomplete beta function. This calculation of the probability of having visited $n \gg 1$ sites at time t is one of our main results. In the low energy limit, $E \ll 1$, $S(x)$ becomes [37]

$$S(x) \simeq (\beta + 1/2)(x - 1)^2, \quad (8)$$

in agreement with Eq. (7) in the limit $|x - 1| \ll 1$ (i.e., in the Gaussian vicinity of $n = \langle n \rangle$). Notably, Eq. (8) can also be obtained by using the Fokker-Planck approximation to Eq. (2) (Supplemental Material, Sec. S1C [37]). While the latter aptly captures the variance, see below, it misses the distribution tails [46]. In Fig. 1(a) we find good agreement between the exact result for the distribution [Eq. (4)], time-dependent WKB approximation [Eqs. (7), (8)], and simulations (see also Supplemental Material, Figs. S1 and S2 [37]). Here the exact result and WKB approximation are practically indistinguishable, whereas the low energy approximation can capture only the distribution's Gaussian vicinity. As stated, for $n \gg 1$ the exact result's accuracy rapidly deteriorates due to summation of alternating large terms, making the time-dependent WKB approach highly advantageous in this case [42].

The variance can be computed using the action in the Gaussian vicinity of the distribution [Eq. (8)] [47], which

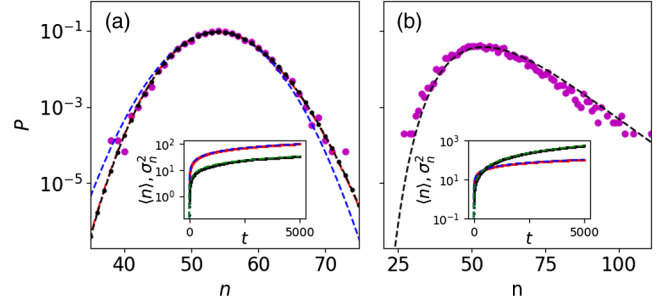


FIG. 1. The probability $P(n, t)$ for $\beta = 1$ and $t = 1500$. (a) No variation in β ($\sigma = 0$). We compare simulations (circles), exact result [black dashed-dotted line, Eq. (4)], WKB approximation [red dashed line, Eq. (7)], and WKB approximation at low energies [blue dashed line, Eq. (8)]. (b) Variability in β with $\sigma = 0.1$: simulations (circles) are compared with a numerical solution of Eq. (9) (dashed line). Insets show $\langle n \rangle$ and σ_n^2 (red and black marks, respectively) versus t , compared with theory (dashed lines).

yields $\sigma_n^2 = \langle n \rangle / |S''(x)|_{x=1} = \langle n \rangle / (1 + 2\beta)$. Thus, the distribution is narrower by a factor of $(1 + 2\beta)$ than that predicted by the naïve mean-field approach above. In the inset of Fig. 1(a) both the average [Eq. (3)] and variance of number of sites agree well with simulations for $\beta = 1$ (see also Supplemental Material, Fig. S2, for $\beta = 0.5$ [37]).

In empirical studies, individual preferences and decisions can affect movement and behavior, hence individuals will *not* have identical movement patterns [48,49]. To account for interindividual variation, we generalize our model by allowing different β values across individuals. Assuming β is sampled from a normal distribution $\mathcal{N}(\beta_0, \sigma^2)$ with mean β_0 and variance $\sigma^2 \ll 1$ (indicating the interindividual variability in β around β_0 , see empirical results analysis below), $P_n(t)$ satisfies

$$P(n, t) = \frac{1}{\sqrt{2\pi\sigma^2}} \int_{-\infty}^{\infty} P_\beta(n, t) e^{-\frac{(\beta-\beta_0)^2}{2\sigma^2}} d\beta, \quad (9)$$

where $P_\beta(n, t)$ is the probability at a given β , given by Eq. (7). Although analytical progress is possible only in the limit of small σ (Supplemental Material, Sec. S1D [37]), Eq. (9) can generally be solved numerically [Figs. 1(b), S2(b) of [37]]. Notably, we checked that while interindividual variability almost does not affect the mean number of sites, it strongly affects the variance of the number of sites (Supplemental Material, Fig. S3 [37]).

Statistics of number of visits to a site.—Having computed the statistics of number of sites, we now turn to study the probability $W_i(m_i, t)$ of having m_i visits at time t to an already visited site i , which follows

$$\frac{\partial W_i}{\partial t} = (1 - P_{\text{new}})[\Pi_i(m_i - 1)W_i(m_i - 1, t) - \Pi_i(m_i)W_i(m_i, t)], \quad (10)$$

where P_{new} and Π_i are given by Eq. (1). Here the initial conditions are $m_i(t = t_i) = 1$, where t_i is the first time site i was visited and is a stochastic variable governed by Eq. (2). Below, we focus on the limit $t \gg t_i \geq 1$ where $P_{\text{new}} \rightarrow 0$ [50], and approximate t_i by its average (as evaluated from data). In general, Π_i depends on the number of visits to other sites; thus Eq. (10) couples between different sites. Moreover, the dependence on previous visits makes this a non-Markovian evolution equation [19,51].

The case of $\alpha = 1$.—Here $\sum_i m_i = t$, i.e., the total number of visits to all sites equals the total number of time steps t , which yields $\Pi_i(m_i) = m_i/t$. In addition, for $P_{\text{new}} \simeq 0$, Eq. (10) is solved by $W_i(m_i, t) = t_i t^{-m_i} (t - t_i)^{m_i - 1}$, with average and variance of $\langle m_i \rangle = t/t_i$, and $\sigma_{m_i}^2 = \langle m_i^2 \rangle - \langle m_i \rangle^2 = t(t - t_i)/t_i^2 \simeq t^2/t_i^2$.

The case of $\alpha \neq 1$.—For $\alpha < 1$, we *a priori* assume that $\sum_{j=1}^{(n)} \langle m_j \rangle^\alpha \sim t^\xi$, where ξ is *a priori* unknown and satisfies $\alpha < \xi < 1$. The average number of visits to any site i can then be shown to asymptotically follow $\langle m_i \rangle \sim t^{(1-\xi)/(1-\alpha)} [1 + \mathcal{O}(t^{\xi-1})]$. Plugging this back into the sum over $\langle m_j \rangle^\alpha$ we find that $\xi = \xi_0(1 + \epsilon)$, where $\xi_0 = (1 + \alpha\beta)/(1 + \beta)$ and $\epsilon \ll 1$ is an unknown function of α, β . For $1 - \alpha \gg \epsilon$ [$\beta = \mathcal{O}(1)$], we further find $\langle m_i \rangle \sim t^{\beta/(1+\beta)}$, independent of α ; yet, the condition $1 - \alpha \gg \epsilon$ breaks down as $\alpha \rightarrow 1$. Importantly, in the limit $t \gg 1$, for any $\alpha < 1$ we find that all sites scale similarly with time. In contrast, for $\alpha > 1$ not all sites scale similarly with time. Here $\langle m_i \rangle \simeq t$ for $i = 1$, while $\langle m_i \rangle \simeq C_i [1 + \mathcal{O}(t^{1-\alpha})]$ for $i > 1$, where $C_i = C_i(t_i)$ is a constant. In the Supplemental Material [37], Sec. S2A-C, and Figs. S4, S5 we provide a rigorous proof of the above calculations. Also, in Sec. S2D and Fig. S6 we numerically corroborate the scaling of $\langle m_i \rangle$ and $\sigma_{m_i}^2$ on time for different α and sites, while in Sec. S2E and Fig. S7, we numerically study the statistics of the visits to the first visited site versus α [37].

These results reveal a phase transition at $\alpha = 1$ (see also Supplemental Material, Sec. S2F [37]), where for weak PR ($\alpha < 1$) the frequency of visits to the most visited site $f_1 \equiv \langle m_1 \rangle / \sum_{j=1}^{(n)} \langle m_j \rangle$ is only a small fraction of the total number of visits, while for strong PR ($\alpha > 1$) f_1 approaches 1 as t is increased and site 1 dominates [Fig. 2(a)]. Importantly, in addition to the phase transition for f_1 , the next most visited sites (f_k , for $k = 2, 3, \dots$) peak around $\alpha = 1$ (Figs. 2(b), S8 [37]). Here, for $\alpha < 1$ the visitation frequencies to all sites become similar, while for $\alpha > 1$ these tend to zero.

Movement of fruit bats.—To study the relevance of our model for real-life systems and to obtain insights into the phase transition, we compare our predictions to resource use patterns and visitation dynamics of wild fruit bats tracked by ATLAS during winter and summer [52]. In Figs. 3(a)–3(b) we fit the mean and variance of the number of visited sites (fruit trees) as a function of the number of

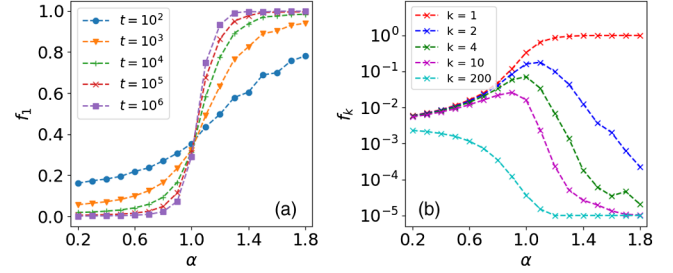


FIG. 2. (a) The average frequency of visits to the most visited site f_1 versus α , for $\beta = 1$ (simulations). Each curve corresponds to a given number of visits t (see legend). (b) Semi-log plot of f_k versus α for different sites (see legend), for $\beta = 1$ and $t = 10^5$.

movement steps (defined here as distinguishable movement between trees [37]) to our theory [53]. We find that during the summer β_0 and σ are higher than during the winter, entailing a lower rate of visits to new sites (higher levels of conformity) and larger interindividual variability, respectively. Notably, our results suggest interindividual variability in both summer and winter. In Figs. 3(c)–3(d) we show that during summer $\langle m_1 \rangle \sim t^{0.97}$ and $\langle m_2 \rangle \sim t^{0.99}$, which matches the theory for $\alpha = 1$. In contrast, during winter

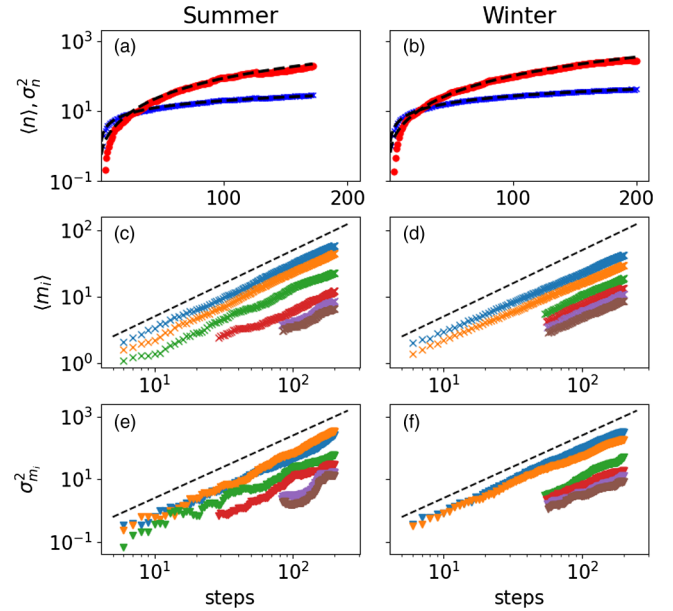


FIG. 3. (a)–(b) The mean (blue marks) and variance (red marks) of the number of sites visited by bats during summer and winter, compared to theoretical prediction (black dashed lines), with fitted values of $\beta_0 = 0.71$ and $\sigma = 0.21$ in (a), and $\beta_0 = 0.53$ and $\sigma = 0.16$ in (b). These are averaged over an ensemble of 38 (a) and 53 (b) bats. (c)–(d) The mean number of visits $\langle m_i \rangle$ to the six most visited sites, $i = 1, \dots, 6$ from top to bottom (different colors mark different sites), averaged over the same ensembles as in (a) and (b). Black dashed lines $\langle m_i \rangle \sim t$ correspond to the theoretical prediction for $\alpha = 1$. (e)–(f) Variance of the number of visits $\sigma_{m_i}^2$ to the same six sites, averaged over the same ensembles for summer (e) and winter (f). Black dashed lines $\sigma_{m_i}^2 \sim t^2$ correspond to the theoretical prediction for $\alpha = 1$.

$\langle m_1 \rangle \sim t^{0.89}$ and $\langle m_2 \rangle \sim t^{0.87}$ which is consistent with α values slightly below 1. Moreover, $\langle m_i \rangle$ versus t_i agrees with our theoretical predictions [see Figs. 3(e)–3(f), Sec. S2D and Fig. S9 also for the dependence of $\sigma_{m_i}^2$ on time [37]]. These seasonal differences may be attributed to the fact that bats during the summer feed of highly abundant and palatable fruits—mulberries or figs with high levels of sugar content—and hence do not need to explore for feeding alternatives (high β_0) and can strongly rely on a limited number of sites ($\alpha = 1$). In contrast, during winter there is less motivation to return to less favorable fruits (chinaberries) and a higher motivation to explore alternative trees, such as nonseasonal (unpredictable) fruit from the Ficus family.

In light of the phase transition at $\alpha = 1$, and in agreement with experimental results, we hypothesize that in animal movement the value of α will tend towards 1. This maximizes the frequencies of visits to preferred sites [Fig. 2(b)], yet avoids an exclusive choice of a preferred site which occurs at $\alpha > 1$ [see Fig. 2(a)]. In this manner the animal combines intensive search patterns (committing to a few sites) with extensive searches (returning to all sites with some probability), a balance which is essential to optimize between energy expenditure and risk management [22,54,55]. Indeed, for fruit bats we find $\alpha \approx 1$, and similar results were obtained for humans [24] and monkeys [31]. Furthermore, the strategy of avoiding an exclusive site resembles bet-hedging strategies, e.g., bacterial persistence [56]. In addition, the value of α may be correlated to the total number of known sites: for large β_0 (few sites, summer) the bats will show stronger PR, while for smaller β_0 (more sites, winter) the strategy may tend towards a more uniform visitation rate to all trees (weaker PR).

More generally, we expect our results to also provide key insights into revisit dynamics in other areas like human mobility [57–59], COVID-19 spread [60], human migration [61], and languages dynamics [62].

O.V. and M.A. were supported by the Israel Science Foundation Grant No. 531/20. M. A. was also supported by the Humboldt Research Fellowship for Experienced Researchers of the Alexander von Humboldt Foundation. Fieldwork with ATLAS was funded by the Minerva Foundation, the Minerva Center for Movement Ecology, and Grants No. ISF-1259/09, No. ISF-965/15, and No. GIF 1316/15 to R. N. Finally, we thank Yoav Bartan, Anat Levi, David Shohami, and other members of the Minerva Center for Movement Ecology for their valuable help with fieldwork.

*To whom all correspondence should be addressed. michael.assaf@mail.huji.ac.il.

[1] R. Nathan, W.M. Getz, E. Revilla, M. Holyoak, R. Kadmon, D. Saltz, and P.E. Smouse, A movement ecology paradigm for unifying organismal movement research, *Proc. Natl. Acad. Sci. U.S.A.* **105**, 19052 (2008).

[2] V. Grimm and S.F. Railsback, *Individual-Based Modeling and Ecology* (Princeton University Press, Princeton, 2005), Vol. 8.

[3] R. Metzler, J.-H. Jeon, A.G. Cherstvy, and E. Barkai, Anomalous diffusion models and their properties: Non-stationarity, non-ergodicity, and ageing at the centenary of single particle tracking, *Phys. Chem. Chem. Phys.* **16**, 24128 (2014).

[4] E. Lourie, I. Schiffner, S. Toledo, and R. Nathan, Memory and conformity, but not competition, explain spatial partitioning between two neighboring fruit bat colonies, *Front. Ecol. Evol.* **9**, 732514 (2021).

[5] E. Gurarie, C. Bracis, M. Delgado, T.D. Meckley, I. Kojola, and C.M. Wagner, What is the animal doing? Tools for exploring behavioural structure in animal movements, *J. Anim. Ecol.* **85**, 69 (2016).

[6] W.F. Fagan, M.A. Lewis, M. Auger-Méthé, T. Avgar, S. Benhamou, G. Breed, L. LaDage, U.E. Schlägel, W.-w. Tang, Y.P. Papastamatiou *et al.*, Spatial memory and animal movement, *Ecol. Lett.* **16**, 1316 (2013).

[7] C. Bracis, E. Gurarie, B.V. Moorter, and R.A. Goodwin, Memory effects on movement behavior in animal foraging, *PLoS One* **10**, e0136057 (2015).

[8] M.A. Lewis, W.F. Fagan, M. Auger-Mth, J. Frair, J.M. Fryxell, C. Gros, E. Gurarie, S.D. Healy, and J.A. Merkle, Learning and animal movement, *Front. Ecol. Evol.* **9**, 441 (2021).

[9] L. Polansky, W. Kilian, and G. Wittemyer, Elucidating the significance of spatial memory on movement decisions by African Savannah elephants using state–space models, *Proc. R. Soc. B* **282**, 20143042 (2015).

[10] N. Ranc, P.R. Moorcroft, F. Ossi, and F. Cagnacci, Experimental evidence of memory-based foraging decisions in a large wild mammal, *Proc. Natl. Acad. Sci. U.S.A.* **118**, e2014856118 (2021).

[11] A. Goldshtein, M. Handel, O. Eitan, A. Bonstein, T. Shaler, S. Collet, S. Greif, R.A. Medellín, Y. Emek, A. Korman *et al.*, Reinforcement learning enables resource partitioning in foraging bats, *Curr. Biol.* **30**, 4096 (2020).

[12] S. Toledo, D. Shohami, I. Schiffner, E. Lourie, Y. Orchan, Y. Bartan, and R. Nathan, Cognitive map–based navigation in wild bats revealed by a new high-throughput tracking system, *Science* **369**, 188 (2020).

[13] J. Nauta, Y. Khaluf, and P. Simoens, Hybrid foraging in patchy environments using spatial memory, *J. R. Soc. Interface* **17**, 20200026 (2020).

[14] A.R. Krochmal, T.C. Roth, and N.T. Simmons, My way is the highway: The role of plasticity in learning complex migration routes, *Anim. Behav.* **174**, 161 (2021).

[15] J.M. Morales, D.T. Haydon, J. Frair, K.E. Holsinger, and J.M. Fryxell, Extracting more out of relocation data: Building movement models as mixtures of random walks, *Ecology* **85**, 2436 (2004).

[16] T. Patterson, L. Thomas, C. Wilcox, O. Ovaskainen, and J. Matthiopoulos, State-space models of individual animal movement, *Trends Ecol. Evol.* **23**, 87 (2008).

[17] L. Riotte-Lambert, S. Benhamou, and S. Chamailé-Jammes, How memory-based movement leads to nonterritorial spatial segregation, *Am. Nat.* **185**, E103 (2015).

- [18] S. Hod and U. Keshet, Phase transition in random walks with long-range correlations, *Phys. Rev. E* **70**, 015104(R) (2004).
- [19] G.M. Schütz and S. Trimper, Elephants can always remember: Exact long-range memory effects in a non-Markovian random walk, *Phys. Rev. E* **70**, 045101(R) (2004).
- [20] R. Nathan *et al.*, Big-data approaches lead to increased understanding of the ecology of animal movement, *Science* **375**, eabg1780 (2022).
- [21] M. R. Evans and S. N. Majumdar, Diffusion with Stochastic Resetting, *Phys. Rev. Lett.* **106**, 160601 (2011).
- [22] O. Berger-Tal and S. Bar-David, Recursive movement patterns: Review and synthesis across species, *Ecosphere* **6**, 1 (2015).
- [23] M. R. Evans, S. N. Majumdar, and G. Schehr, Stochastic resetting and applications, *J. Phys. A* **53**, 193001 (2020).
- [24] C. Song, T. Koren, P. Wang, and A.-L. Barabási, Modelling the scaling properties of human mobility, *Nat. Phys.* **6**, 818 (2010).
- [25] D. Boyer and C. Solis-Salas, Random Walks with Preferential Relocations to Places Visited in the Past and their Application to Biology, *Phys. Rev. Lett.* **112**, 240601 (2014).
- [26] A. Falcón-Cortés, D. Boyer, L. Giuggioli, and S. N. Majumdar, Localization Transition Induced by Learning in Random Searches, *Phys. Rev. Lett.* **119**, 140603 (2017).
- [27] H. Meyer and H. Rieger, Optimal Non-Markovian Search Strategies with n -Step Memory, *Phys. Rev. Lett.* **127**, 070601 (2021).
- [28] O. Benichou, R. Voituriez *et al.*, Self-Interacting Random Walks: Aging, Exploration and First-Passage Times, [arXiv:2109.13127](https://arxiv.org/abs/2109.13127) [Phys. Rev. X (to be published)].
- [29] D. Boyer and J. C. R. Romo-Cruz, Solvable random-walk model with memory and its relations with Markovian models of anomalous diffusion, *Phys. Rev. E* **90**, 042136 (2014).
- [30] D. Campos and V. Méndez, Recurrence time correlations in random walks with preferential relocation to visited places, *Phys. Rev. E* **99**, 062137 (2019).
- [31] D. Boyer, M. C. Crofoot, and P. D. Walsh, Non-random walks in monkeys and humans, *J. R. Soc. Interface* **9**, 842 (2012).
- [32] P. L. Krapivsky, S. Redner, and F. Leyvraz, Connectivity of Growing Random Networks, *Phys. Rev. Lett.* **85**, 4629 (2000).
- [33] Similar growth rates appear in self-inhibitory gene regulatory networks, where a protein inhibits its own growth, see, e.g., Refs. [34,35].
- [34] Y. Dublanche, K. Michalodimitrakis, N. Kümmerer, M. Foglierini, and L. Serrano, Noise in transcription negative feedback loops: Simulation and experimental analysis, *Mol. Syst. Biol.* **2**, 41 (2006).
- [35] E. Roberts, S. Be'er, C. Bohrer, R. Sharma, and M. Assaf, Dynamics of simple gene-network motifs subject to extrinsic fluctuations, *Phys. Rev. E* **92**, 062717 (2015).
- [36] In the Supplemental Material, Sec. S1B [37] we develop an alternative generating function approach, and Eq. (2) becomes a fractional integro-differential equation, solvable in specific cases.
- [37] See Supplemental Material at <http://link.aps.org/supplemental/10.1103/PhysRevLett.128.148301> for more details and additional results from our analysis, which includes Refs. [59–62].
- [38] M. Abramowitz and I. A. Stegun, *Handbook of Mathematical Functions with Formulas, Graphs, and Mathematical Tables*, Ninth Dover Printing, Tenth GPO Printing ed. (Dover, New York, 1964).
- [39] G. B. Arfken and H. J. Weber, *Mathematical methods for physicists* (1999).
- [40] G. G. Kwiecinski and T. A. Griffiths, *Rousettus egyptiacus*, *Mammalian species* **611**, 1 (1999).
- [41] P. R. Gupte, C. E. Beardsworth, O. Spiegel, E. Lourie, S. Toledo, R. Nathan, and A. I. Bijleveld, A guide to pre-processing high-throughput animal tracking data, *bioRxiv* (2020).
- [42] M. Assaf and B. Meerson, Spectral formulation and WKB approximation for rare-event statistics in reaction systems, *Phys. Rev. E* **74**, 041115 (2006).
- [43] M. I. Dykman, E. Mori, J. Ross, and P. Hunt, Large fluctuations and optimal paths in chemical kinetics, *J. Chem. Phys.* **100**, 5735 (1994).
- [44] V. Elgart and A. Kamenev, Rare event statistics in reaction-diffusion systems, *Phys. Rev. E* **70**, 041106 (2004).
- [45] M. Assaf and B. Meerson, WKB theory of large deviations in stochastic populations, *J. Phys. A* **50**, 263001 (2017).
- [46] M. Assaf and B. Meerson, Spectral theory of metastability and extinction in a branching-annihilation reaction, *Phys. Rev. E* **75**, 031122 (2007).
- [47] M. Assaf and B. Meerson, Extinction of metastable stochastic populations, *Phys. Rev. E* **81**, 021116 (2010).
- [48] N. J. Dingemans, C. Both, P. J. Drent, K. Van Oers, and A. J. Van Noordwijk, Repeatability and heritability of exploratory behaviour in great tits from the wild, *Anim. Behav.* **64**, 929 (2002).
- [49] N. J. Dingemans and N. A. Dochtermann, Quantifying individual variation in behaviour: Mixed-effect modelling approaches, *J. Anim. Ecol.* **82**, 39 (2013).
- [50] In this case, Eq. (10) is similar to the master equation in Ref. [25]. Yet, they only consider the case of $\beta = 0$.
- [51] P. Hänggi and H. Thomas, Time evolution, correlations, and linear response of non-Markov processes, *Z. Phys. B* **26**, 85 (1977).
- [52] To have proper statistics and ensure no significant resource depletion, we analyze 10-day periods for each bat. Moreover, we do not explicitly consider spatial effects in our model; see the Supplemental Material [37] Sec. S3 for justification. For details on ATLAS see Ref. [12], and on the species, seasonality, and the segmentation and fitting procedures, see Supplemental Material [37] Sec. S3.
- [53] The power-law dependence of the mean has also been experimentally observed in humans [24] and monkeys [31]; yet, these studies did not analyze fluctuations around $\langle n \rangle$.
- [54] K. Garg and C. T. Kello, Efficient Lévy walks in virtual human foraging, *Sci. Rep.* **11**, 5242 (2021).
- [55] B. C. Nolting, T. M. Hinkelman, C. E. Brassil, and B. Tenhumberg, Composite random search strategies based

- on non-directional sensory cues, *Ecol. Complexity* **22**, 126 (2015).
- [56] N. Q. Balaban, J. Merrin, R. Chait, L. Kowalik, and S. Leibler, Bacterial persistence as a phenotypic switch, *Science* **305**, 1622 (2004).
- [57] F. Schlosser and D. Brockmann, Finding disease outbreak locations from human mobility data, *EPJ Data Sci.* **10**, 52 (2021).
- [58] D. do Couto Teixeira, J. M. Almeida, and A. C. Viana, On estimating the predictability of human mobility: The role of routine, *EPJ Data Sci.* **10**, 49 (2021).
- [59] M. Schläpfer, L. Dong, K. O'Keefe, P. Santi, M. Szell, H. Salat, S. Anklesaria, M. Vazifeh, C. Ratti, and G. B. West, The universal visitation law of human mobility, *Nature (London)* **593**, 522 (2021).
- [60] A. Galeazzi, M. Cinelli, G. Bonaccorsi, F. Pierri, A. L. Schmidt, A. Scala, F. Pammolli, and W. Quattrociocchi, Human mobility in response to covid-19 in France, Italy and UK, *Sci. Rep.* **11**, 13141 (2021).
- [61] G. Chi, F. Lin, G. Chi, and J. Blumenstock, A general approach to detecting migration events in digital trace data, *PLoS One* **15**, e0239408 (2020).
- [62] H. Watanabe, Empirical observations of ultraslow diffusion driven by the fractional dynamics in languages, *Phys. Rev. E* **98**, 012308 (2018).